Protein Science (1996), 5:24–33. Cambridge University Press. Printed in the USA.

Identification of the *Serratia* endonuclease dimer: Structural basis and implications for catalysis

MITCHELL D. MILLER AND KURT L. KRAUSE

Department of Biochemical and Biophysical Sciences, University of Houston, Houston, Texas 77204-5934

(RECEIVED August 15, 1995; ACCEPTED October 13, 1995)

Abstract

The *Serratia* endonuclease is an extracellularly secreted enzyme capable of cleaving both single- and double-stranded forms of DNA and RNA. It is the first member of a large class of related and usually dimeric endonucleases for which a structure is known. Using X-ray crystallography, the structure of monomer of this enzyme was reported by us previously (Miller MD et al., 1994, *Nature Struct Biol 1*:461–468). We now confirm the dimeric nature of this enzyme through light-scattering experiments and identify the physiologic dimer interface through crystal packing analysis. This dimerization occurs through an isologous twofold interaction localized to the carboxy-terminal subdomain of the enzyme. The dimer is a prolate ellipsoid with dimensions 30 Å × 35 Å × 90 Å. The dimer interface is flat and contains four salt links, several hydrogen bonds, and nonpolar interactions. Buried water is prominent in this interface and it includes an unusual "cubic" water cluster. The position of the two active sites in the dimer suggests that they can act independently in their cleavage of DNA, but have a geometrical advantage in attacking substrate relative to the monomer.

Keywords: dimer interface; endonuclease; protein–protein interactions; protein structure; X-ray crystallography

Serratia marcescens endonuclease is an extracellularly secreted enzyme of 26,700 Da that is sugar nonspecific, i.e., capable of cleaving both DNA and RNA, and able to cleave both double- and single-stranded forms of nucleic acid (Eaves & Jeffries, 1963; Yonemura et al., 1983; Ball et al., 1987). It catalyzes the production of 5′ monophosphate-terminated oligonucleotides, possesses a requirement for divalent magnesium, and has a pH optimum of 8 (Nestle & Roberts, 1969; Biedermann et al., 1989). Many of its properties resemble those of DNase I, but the *Serratia* endonuclease is a much faster enzyme, with a specific activity more than 15 times greater (Friedhoff et al., 1994b).

The *Serratia* endonuclease belongs to a group of major sugar nonspecific nucleases that have been found in several different species from both prokaryotic and eukaryotic organisms. Homologous eukaryotic nucleases include mitochondrial nucleases such as NUC1 from *Saccharomyces cerevisiae* and endonuclease G from *Bos taurus* (Fraser & Low, 1993). These two nucleases are homodimers, with monomer M_r of about 30 kDa, and they are associated with the inner membrane of mitochondria (Vincent et al., 1988; Côté & Ruiz-Carrillo, 1993). Another nuclease, a 29-kDa sugar-nonspecific nuclease from *Anabaena* sp. PCC 7120 (Muro-Pastor et al., 1992), has also been shown to contain significant sequence similarity to *Serratia* endonuclease. There is evidence from Southern blotting and nuclease gel assays that this nuclease is widespread in heterocyst-forming cyanobacteria (Muro-Pastor et al., 1994). Although all of the nucleases of this group are sugar nonspecific, some of them show a preference for cleavage of DNA in sequences that are enriched for certain nucleotides. For example, bovine endonuclease G prefers to cleave DNA in long regions of dC·dG DNA (Côté et al., 1989) and *Serratia* endonuclease has been found to act in a similar but less pronounced fashion (Meiss et al., 1995).

We recently reported the 2.1-Å crystal structure of the *Serratia* endonuclease (Miller et al., 1994), and it remains the only member of this group for which three-dimensional structural information is available. In that initial report, we focused on the structural description of the monomer, but most researchers feel that this group of endonucleases function as dimers. For the *Serratia* endonuclease, the evidence for this dimerization results primarily from biophysical studies of the enzyme in solution. Analysis of sedimentation velocity experiments performed by Filimonova et al. (1981) on the *Serratia* nuclease suggested that the nuclease is probably composed of a dimer of identical subunits (Friedhoff et al., 1994b). Evidence from gel filtration and dimethyl suberimidate crosslinked SDS-PAGE studies is also consistent with the interpretation of the nuclease as a homodimer (M. Benedik, pers. comm.).

In this report, we offer additional biochemical evidence for the *Serratia* endonuclease dimer based on dynamic light scattering. We review the geometry and energetics of packing within

Reprint requests to: Kurt L. Krause, Department of Biochemical and Biophysical Sciences, University of Houston, Houston, Texas 77204-5934; e-mail: kkrause@uh.edu.

the nuclease crystal. Based on these results, we identify the interface belonging to the *Serratia* endonuclease homodimer. We then present a detailed accounting of the noncovalent interactions that bridge the two monomers and discuss the implications of dimerization on the function of the enzyme.

The study of the structural basis of protein-protein interactions has been the subject of intensive research and review because of its relevance in explaining protein signal transduction and cooperativity (Miller, 1989; Janin & Chothia, 1990; Jones & Thorton, 1995). Therefore, the description of the *Serratia* endonuclease dimer is of value both as the first description of a dimeric sugar nonspecific nuclease, and as another illustration of a detailed dimeric interface in a multisubunit protein.

Table 1. *Light scattering results*[a]

D_T (10^{-13} m^2 s^{-1})	R_H (nm)	M_r (kDa)	Sum of squares	Comments
695.4 (4.1)	3.2 (0.04)	48.7 (0.9)	0.22 (0.08)	Monodisperse[b]

[a] Results are from the average of 20 measurements for 5 mg/mL nuclease in 40 mM Tris, pH 8.2, 100 mM NaCl, 2 mM $MgCl_2$. Numbers in parentheses are the σ_{n-1} values for the averages. The molecular mass is estimated from an empiric relationship based on the typical solution behavior properties of globular proteins. The sum of squares is a measure of the agreement of the experimental results and the auto-correlation function.

[b] A solution is considered monodisperse if the standard deviation of the size distribution is less than 15% of the mean radius measurement.

Results and discussion

Light-scattering experiments

Light-scattering experiments (Schmitz, 1990) conducted under conditions where the nuclease is normally active gave a particle size of 3.2 nm whose derived molecular weight of 48.7 kDa corresponds closely to the expected size of the *Serratia* endonuclease homodimer (Table 1). Similar results have been obtained in other buffer systems with protein concentrations ranging from 1 to 5 mg/mL. These results, combined with previously reported biophysical studies, strongly support a dimeric endonuclease, but they do not identify its structural basis.

Packing of nuclease monomers in the crystallographic unit cell

The *Serratia* nuclease crystallizes with eight nuclease monomers in the unit cell of space group $P2_12_12$ (Fig. 1). Two of these monomers, which we describe as monomer A and monomer B, form the asymmetric unit with the other monomers being crystallographically related to either monomer A or B. There is strong pseudo body-centering in this crystal form, with monomer A and monomer B being related by an approximate translation of (0.5, 0.5, 0.5). In fact, the transformation required to shift the packing into a body-centered lattice would require only that one monomer shift 1.4 Å and rotate 1° about its centroid. This motion would change the space group from $P2_12_12$ to I222.

The combination of the noncrystallographic pseudo body-centering with the crystallographic symmetry of space group $P2_12_12$ results in seven different symmetry axes relating the monomers in the unit cell. The three crystallographic symmetry axes relating monomer A to monomer A and monomer B to monomer B are a twofold parallel to z, and twofold screw axes parallel to x and y. There are four noncrystallographic symmetry axes that relate monomer A to monomer B: the centering translation, twofold axes along x and y, and a twofold screw along z. These seven symmetry elements create 11 unique mono-

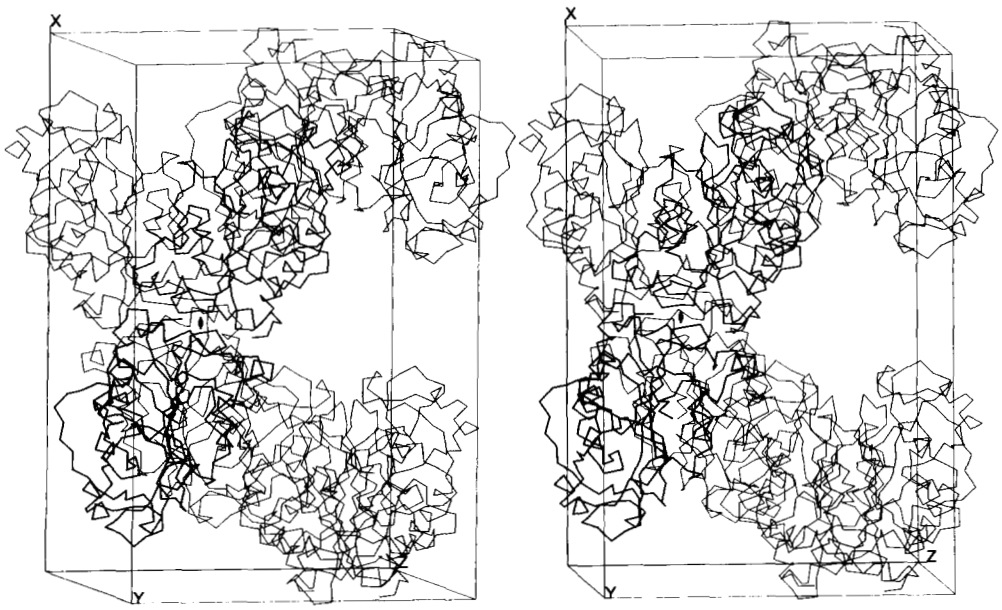

Fig. 1. Stereo-packing diagram of the *Serratia* endonuclease in the $P2_12_12$ lattice viewed along y. The noncrystallographic twofold axis parallel to y, which relates monomers A (black) and B (gray) of the dimeric enzyme, is indicated.

mer:monomer interfaces in the crystal lattice. Three of the interfaces are between molecule A and crystallographically related molecules of A, three are between molecule B and crystallographically related molecules of B, and the remaining five interfaces are between molecule A and a noncrystallographic symmetry related molecule B.

Identification of the dimer interface

A systematic analysis of all 11 monomer:monomer interfaces in the $P2_12_12$ nuclease crystals was done to identify which interface is associated with the physiologic *Serratia* endonuclease dimer (Table 2). Of the six interfaces involving either A:A or B:B interactions, two lack crystal contacts. Specifically, the A:A and B:B interfaces formed by the crystallographic twofold screw-axis along x do not contain any interactions. The four remaining A:A and B:B interfaces all have minor contact regions containing relatively small amounts of buried surface area, that is, less than 3% of the total surface area of the monomer. Therefore, the nuclease dimer is not produced by the action of a crystallographic symmetry element.

The five remaining interfaces involve monomer A interacting with monomer B and can be divided into three groups. The first group contains one interface formed between monomers of A and B resulting from the noncrystallographic pseudo body-centering transformation found in this crystal. This relation results in no protein-protein contacts. The second group contains the three interfaces produced by the noncrystallographic twofold along x and the noncrystallographic twofold screw axis along z. This group displays only minor contact surfaces and small, but unfavorable, complementary energies of 2, 16, and 27 kcal/mol, respectively. The third group contains the interface produced by the action of a noncrystallographic twofold axis located along y. This axis splits two abutted nuclease monomers directly at the midpoint of their interacting surface (Fig. 1). This interface buries more than 2,000 Å^2 of monomer surface area.

Interface surface area and energetics

The A:B interface produced by the action of the noncrystallographic twofold along the y axis represents the physiological dimer interface because it contains a large surface area of complimentary charge and shape that allows the formation of a single globular entity that can act as a functional enzyme.

Each monomer is covered with roughly 10,000 Å^2 of surface area. Dimerization across the noncrystallographic twofold along y involves 2,016 Å^2 (or 1,008 Å^2 per monomer) and reduces the solvent-accessible surface area by 10.4%. This is at least twice the buried surface of any other interface listed in Table 2 and is, therefore, likely to be significant structurally (Janin et al., 1988; Jones & Thorton, 1995). The shape of the dimer produced in this manner is a smoothly varying prolate ellipsoid with approximate overall dimensions of 30 Å × 35 Å × 90 Å (Fig. 2A, Kinemage 1). This kind of closed shape is consistent with what is expected for a soluble, globular protein (Janin et al., 1988; Creighton, 1993). In contrast, the monomer in isolation displays a dramatically flat region on its molecular surface (Fig. 2B). None of the other packing interfaces located in the *Serratia* endonuclease unit cell would bury this flat region of the monomer and none would produce a dimer with a smooth globular shape.

We have calculated interaction energies at all of the packing interfaces in the *Serratia* endonuclease unit cell. The interaction energy at the proposed dimer interface is far more favorable than similar interaction energies calculated for the other interfaces present in the crystal. A survey of Table 2 reveals that the proposed dimer interface has an overall interchain energy, which is a combination of the van der Waals and electrostatic energy, of −249 kcal/mol for the noncrystallographic twofold interface along y. The second most favorable interaction listed is only

Table 2. *Molecular interfaces in the $P2_12_12$ nuclease crystal*

Symmetry relation	Surface area (Å^2)[a]	Buried surface[b]	E-total[c] (kcal/mol)	E-total interchain	E(VDW) interchain	E(ELEC) interchain
NUCA alone	9,702		−4,170.6			
NUCB alone	9,660		−4,088.4			
NCS A:B twofold y	17,346	2,016 (10.4%)	−8,507.7	−248.8	−124.3	−124.5
NCS A:B twofold x	18,572	790 (4.1%)	−8,256.9	2.1	−48.8	50.9
NCS A:B two-screw z	18,398	964 (4.9%)	−8,243.5	15.5	−43.7	59.2
NCS A:B two-screw z	18,351	1,011 (5.2%)	−8,232.3	26.6	−41.4	68.0
NCS A:B Pseudo I center	19,360	2 (0.01%)	−8,193.5	65.5	0.0	65.5
Cryst A:A twofold z	18,900	504 (2.6%)	−8,276.1	65.1	−20.3	85.4
Cryst A:A two-screw x	19,400	4 (0.02%)	−8,253.7	87.5	−1.0	88.4
Cryst A:A two-screw y	18,970	434 (2.2%)	−8,239.4	101.7	−16.4	118.1
Cryst B:B twofold z	19,018	301 (1.6%)	−8,111.8	65.0	−9.7	74.7
Cryst B:B two-screw x	19,303	16 (0.1%)	−8,088.8	87.9	−1.0	88.9
Cryst B:B two-screw y	18,774	545 (2.8%)	−8,090.8	85.9	−21.3	107.2

[a] Solvent-accessible surface areas (Å^2) for each monomer and for the pairwise complexes present in the crystal lattice were calculated using the grid based method in X-PLOR version 3.1 (Brünger, 1992).

[b] Total amount of surface area (Å^2) buried for each complex is the difference between the surface area of the two monomers in isolation and the surface area of complex.

[c] All energy values are in kcal/mol and were calculated in X-PLOR version 3.1 using the Engh and Huber (1991) parameter set parhcsdx.pro with no nonbonded cutoff, a protein dielectric of 2.0, and nuclease coordinates with solvent atoms removed.

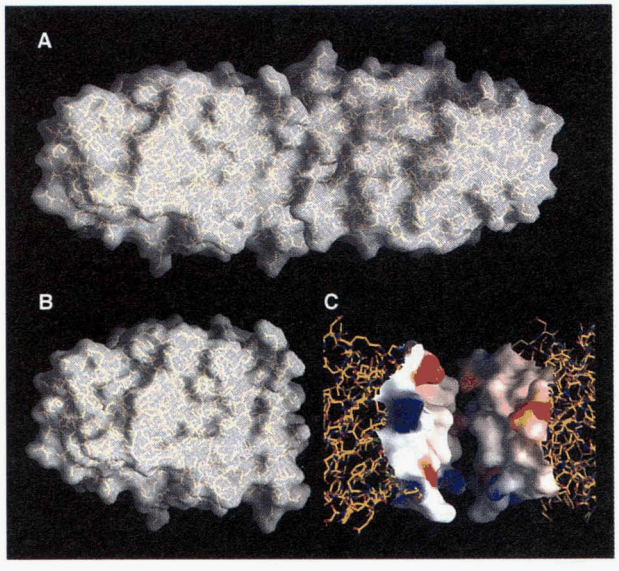

Fig. 2. The molecular surface of the nuclease dimer forms a smoothly varying prolate ellipsoid (**A**). The monomer has a remarkably flat surface that is buried upon dimerization (**B**). When the dimer is pulled apart and the electrostatic potential is mapped onto the molecular surface of the interface, the shape and charge complementarity is evident (**C**). This figure was created with GRASP (Nicholls & Honig, 1992).

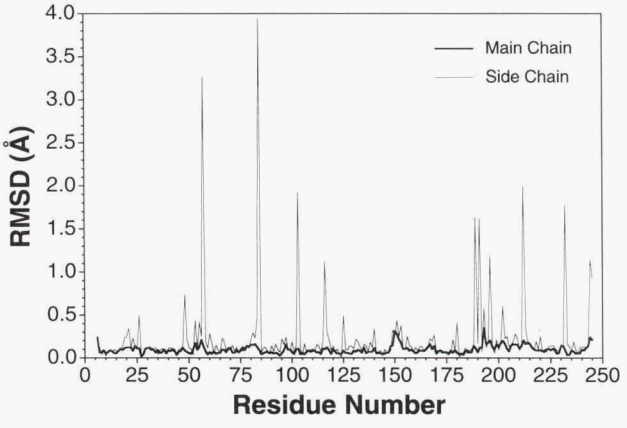

Fig. 3. RMS difference between monomer A and monomer B in the asymmetric unit of the unit cell. Backbones are very similar with some side chains built in alternate conformers. Note that the two monomers were refined independently and have never been averaged or subjected to noncrystallographic restraints or constraints.

2 kcal/mol. These calculations provide valuable insight into the relative strengths of the interactions at the packing interfaces, even though solvation effects have not been included and they lack an entropy component and are, therefore, not free energies.

The remarkable degree to which the dimerization surfaces are complimentary electrostatically as well as sterically is illustrated in Figure 2C and Kinemage 1, where the dimer is pulled apart, exposing the molecular surface with overlaid electrostatics. For every protrusion on the monomer molecular surface in the dimer interface, there exists a complementary invagination, and for every area of positive electrostatic charge, there exists in the dimer interface a matching area of negative electrostatic charge (Miller, 1989).

Thermal factor analysis

The isotropic temperature factors in the core of the putative dimer interface are quite low. Within 7.5 Å of the center of this region they average 4.8 $Å^2$. This compares favorably to an average of 4.7 $Å^2$ for the thermal parameters found within 7.5 Å of the center of the monomers. For comparison, the mean isotropic temperature factor for all protein atoms in the monomer is 10.5 $Å^2$. The small temperature factors within the dimer interface indicate that this region is similarly ordered as the interior of the monomer, and is another indication that our choice for the physiological dimer interface is correct (Jones & Thorton, 1995).

Fidelity of the twofold

The *Serratia* nuclease dimer is generated by the action of a noncrystallographic twofold axis acting on one monomer. The fidelity of this twofold relationship for the *Serratia* nuclease dimer is high (Fig. 3). The superimposed monomers have RMS differences of 0.1 Å and 0.4 Å for the main chain and all protein atoms, respectively. Most of the differences between the two monomers are localized to side chains on the surface of the molecules. Difference maps suggest that these differences result from side chains that could have been represented as alternate conformers or from flexible surface side chains of residues like lysine. Dimerization involving a twofold relation of this sort is common, and it is appealing because of its simplicity (Klotz et al., 1970). A few homodimeric proteins, like hexokinase, are involved in heterologous interactions without a twofold symmetry axis, but they are rare (Matthews & Bernhard, 1973).

General description of the dimer interface

The dimer interface region is confined to the carboxy subdomain of the enzyme, previously defined as extending from residue 115 to the carboxy-terminus (Miller et al., 1994). Each monomer contributes two loops, two helices, and its carboxy-terminus to this interface (Fig. 4, Kinemage 1). The first loop is located between helix H1 and strand 4 of the central β-sheet and contains residues 135–140. The second loop, which contains residues 177–184, is located between strands 5 and 6 of the central β sheet. Each loop from one monomer primarily interacts with the symmetry related loop from the other monomer.

Helices 3 and 4 and the carboxy-terminus are also involved in the formation of the dimer interface. Helix 3, residues 224–231, from one monomer interacts with the helix 4, residues 236–242, and the carboxy-terminus of the other monomer. These helices are loosely packed, with their helical axes about 7–8 Å apart. They are oriented with their axes roughly 50° relative to each other, placing it in the 4-4 helical packing class of Chothia et al. (1981). The closest packed atoms are the carbonyl oxygen of Ser 229 to the γ-carbon of Leu 239 and the γ-hydroxyl group of Ser 229 to the carbonyl oxygen of Leu 239, with the atoms in both interactions separated by 3.5 Å.

Helix/helix and loop/loop interactions are two important motifs shown to be present in the interfaces of dimeric proteins by Miller (1989). In the case of the *Serratia* endonuclease, both kinds of interactions are present. The shape of the dimerization

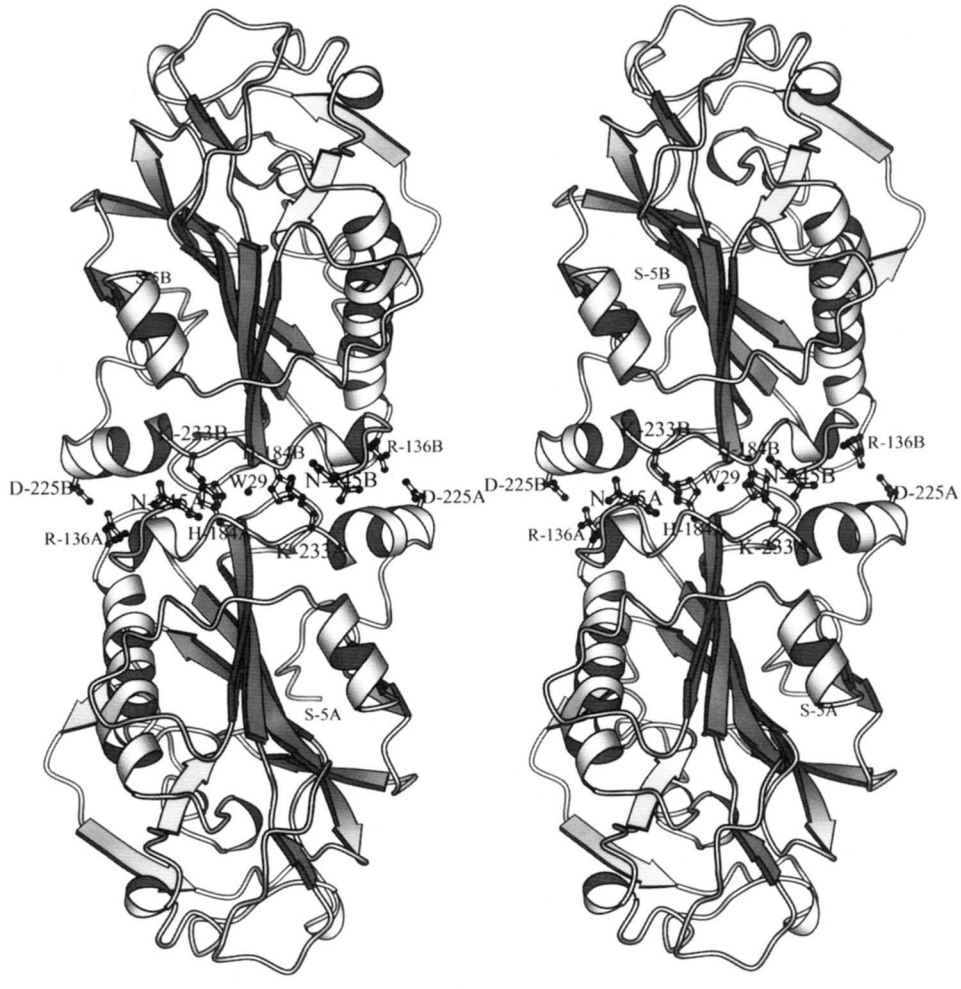

Fig. 4. Schematic MOLSCRIPT (Kraulis, 1991) diagram showing the nuclease dimer with the four salt links and the His-184/H_2O-29 network. Water W-29 is positioned on the noncrystallographic twofold axis.

interaction surface formed by these interactions is generally flat except for complementary invaginations and protrusions. Electrostatic interactions across the interface are complementary as well (Fig. 2C). These findings are all consistent with the expected properties of a dimer interface (Monod et al., 1965; Zielenkiewicz & Rabczenko, 1984; Miller, 1989; Jones & Thorton, 1995).

Noncovalent interactions in the dimer interface

The interface region is stabilized by several strong noncovalent interactions (Table 3). Specifically, there are four salt links and eight direct hydrogen bonds that bridge the two monomers (Kinemage 1). Also, there are 17 hydrogen bonds that contain bridging water molecules, which are termed water-mediated hydrogen bonds in Table 3. Significant numbers of nonpolar interactions are also found across the dimer interface.

The four salt links present in the dimer interface involve eight residues that bridge the opposing monomers. As is evident from Table 3, all of these ionic interactions are symmetric, that is, if a link is seen from molecule A to B, then the same interaction is also seen extending from molecule B to A. Two of the salt links are formed between the ϵ-amino group of lysine 233 in one chain and the α-carboxyl group from the carboxy-terminal residue, asparagine 245, from the other chain (Fig. 4). This is similar to the interactions seen in the α_1/β_2 and α_2/β_1 interfaces in deoxyhemoglobin, where lysine 40 in the α chain interacts with the α-carboxyl of histidine 146 in the β chain (Perutz, 1970a,b). The other two salt links in the nuclease dimer interface occur between the carboxyl group of aspartate 225 and the guanidinium group of arginine 136 from the opposite chain.

The hydrogen bonding network linking the two monomers is extensive. The core of the interface is dominated by interactions bridging His 184 from one monomer to His 184 in the other monomer (Fig. 5A). There are three central water molecules buried in this region that bridge the structural dimer, including one whose oxygen atom is located directly on the twofold axis relating monomer A to monomer B. The oxygen atom of this central water (H_2O-29) has a tetrahedral array of hydrogen bonding neighbors formed by His 184 Nδ1 from both monomers and two other waters (Fig. 5A). The other waters in the core of the interface are also bonded to main-chain amides: H_2O-5 to Tyr B185 and Val B236 and H_2O-8 to Tyr A185 and Val A236. The temperature factors for these waters (H_2O-5, H_2O-8, and H_2O-29) average 3.6 Å^2. This is low, but not appreciably dif-

Table 3. *Intermolecular hydrogen bonds, salt links, and nonbonded contacts in the dimer interface*

Molecule 1			Molecule 2			
Residue	Atom	B (Å^2)	Residue	Atom	B (Å^2)	Distance (Å)
Intermolecular salt links (≤3.5 Å)						
Arg A136	NH1	28.8	Asp B225	OD2	23.6	2.9
Arg A136	NH2	28.5	Asp B225	OD2	23.6	3.1
Asp A225	OD2	23.6	Arg B136	NH1	24.7	2.9
Asp A225	OD2	23.6	Arg B136	NH2	25.1	3.2
Lys A233	NZ	17.7	Asn B245	OT	33.6	2.7
Lys A233	NZ	17.7	Asn B245	O	34.7	3.5
Asn A245	O	29.2	Lys B233	NZ	19.6	3.5
Asn A245	OT	28.7	Lys B233	NZ	19.6	2.8
Intermolecular hydrogen bonds (≤3.5 Å)						
Pro A180	O	6.5	His B184	NE2	6.1	2.6
Ala A181	O	8.6	His B184	NE2	6.1	3.3[a]
Val A182	O	4.0	Asn B183	ND2	4.2	3.1
Val A182	O	4.0	His B184	N	2.2	3.1
Asn A183	ND2	4.2	Val B182	O	4.2	3.0
His A184	N	3.0	Val B182	O	4.2	3.1
His A184	NE2	4.2	Pro B180	O	5.9	2.8
His A184	NE2	4.2	Ala B181	O	7.2	3.2[a]
Water-mediated intermolecular hydrogen bonds (≤3.5 Å)						
Asp A138	OD1	24.4	H_2O-125	OH2	29.4	3.1
Asn A178	OD1	20.9	H_2O-130	OH2	23.1	3.1
Ala A181	O	8.6	H_2O-100	OH2	29.2	3.2
Asn A183	ND2	4.2	H_2O-130	OH2	23.1	3.0
His A184	ND1	5.6	H_2O-29	OH2	5.0	2.8
Tyr A185	N	2.6	H_2O-8	OH2	2.9	3.3
Val A236	N	6.2	H_2O-8	OH2	2.9	3.0
Asp B138	OD1	22.0	H_2O-100	OH2	29.2	3.2
Asn B178	OD1	19.8	H_2O-95	OH2	20.2	3.3
Ala B181	O	7.2	H_2O-125	OH2	29.4	3.1
Asn B183	ND2	4.2	H_2O-95	OH2	20.2	3.0
His B184	ND1	6.4	H_2O-29	OH2	5.0	2.7
Tyr B185	N	3.2	H_2O-5	OH2	3.0	3.1
Val B236	N	6.5	H_2O-5	OH2	3.0	3.1
H_2O-5	OH2	3.0	H_2O-29	OH2	5.0	2.9
H_2O-8	OH2	2.9	H_2O-29	OH2	5.0	2.8
H_2O-95	OH2	20.3	H_2O-130	OH2	23.1	2.9
Nonbonded protein–protein contacts (≤3.5 Å)						
Arg A136	CZ	28.5	Asp B225	OD2	23.6	3.5
Asp A138	OD2	25.6	Ala B181	CB	3.8	3.3
Pro A180	O	6.5	His B184	CE1	6.3	3.2
Ala A181	CB	6.1	Asp B138	OD2	24.4	3.4
Ala A181	C	7.2	His B184	NE2	6.1	3.4
Ala A181	O	8.6	His B184	CD2	6.6	3.2
Val A182	O	4.0	Asn B183	CA	3.5	3.2
Asn A183	CA	3.7	Val B182	O	4.2	3.1
Asn A183	CB	2.9	Val B182	O	4.2	3.5
Asn A183	O	5.5	His B184	CE1	6.3	3.1
His A184	CD2	4.7	Ala B181	O	7.2	3.1
His A184	CE1	5.4	Pro B180	O	5.9	3.2
His A184	CE1	5.4	Asn B183	O	3.9	3.1
His A184	NE2	4.2	Ala B181	C	6.4	3.3
Ser A229	CB	13.9	Glu B239	O	9.6	3.3
Lys A233	NZ	17.7	Asn B245	C	34.0	3.2
Glu A239	O	8.4	Ser B229	CB	14.0	3.3
Leu A240	CD1	11.9	Ala B181	O	7.2	3.5
Asn A245	C	29.2	Lys B233	NZ	19.6	3.3

[a] These hydrogen bonds are about 3° outside the 90° angular cutoff applied for hydrogen bonding.

ferent from the surrounding protein atoms, whose temperature factors average 4.8 Å^2. When these crystals are soaked with K_3IrCl_6, the central water is replaced with iridium and forms the strongest iridium site in the original multiple isomorphous replacement phases.

There is an additional network of eight hydrogen bonds that acts to bridge a large portion of the dimer region (Fig. 5B). These bonds traverse back and forth across the dimer interface and involve main-chain, side-chain, and water-mediated hydrogen bonds. For example, the main-chain amide of His B184 is bonded to the main-chain carbonyl oxygen of Val A182, which then is linked to the amido group on the side chain of Asn B183. The corresponding symmetry related interactions beginning with His A184 are also present, along with two connecting solvent molecules, H_2O-95 and H_2O-130, that bridge the two asparagine side chains. Aside from the central water in the dimer interface, there are several other waters that are involved in the hydrogen bonding network that bridges the dimer. Such water-mediated hydrogen bonds have been seen in the interfaces of many other proteins and they may help to stabilize the interface (for review, see Janin & Chothia, 1990).

In addition to the extensive polar and charged contacts across the interfaces, important hydrophobic interactions are present. There are about 20 nonbonded interactions between protein atoms that are less than 3.5 Å apart, involving 23 residues (Table 3, Kinemage 1). The calculated van der Waals energy is −124 kcal/mol, which is more than twice the van der Waals energy of the other noncrystallographic contact surfaces and over five times the van der Waals energy of the crystallographic contact surfaces (Table 2). About 70% of the solvent-accessible surface buried upon dimerization is hydrophobic. This is similar to the average of 68.1% nonpolar solvent-accessible surface area buried for the 32 nonhomologous dimers analyzed by Jones and Thorton (1995).

An unusual water cluster

The pair of waters mentioned above (H_2O-95 and H_2O-130) have angles between their oxygen atoms and the atoms to which they are hydrogen bonded that are close to 90° (Fig. 5B), strongly deviating from 109.5° expected for a tetrahedral geometry. This type of hydrogen bonding has been observed in theoretical studies of small water clusters where cubic arrays of water molecules are found (Tsai & Jorden, 1993). These cubic structures apparently occur because they allow for the maximum number of hydrogen bonds to be formed in an environment that does not allow for a full extended tetrahedral array of water:water interactions (Savage, 1993).

Implications of the dimerization on nuclease function

We previously identified the *Serratia* endonuclease active site in the large cleft between the long helix, H1, and the long loop that is located between residues 48 and 114 (Miller et al., 1994). This location is consistent with electrostatic calculations, difference density measurements, sequence analysis, and mutagenesis experiments (Muro-Pastor et al., 1992; Friedhoff et al., 1994a; Miller et al., 1994).

Upon dimerization, this region of the protein remains unobstructed and completely open to solvent. The two active site regions face into solution on opposite sides of the dimer (Fig. 6).

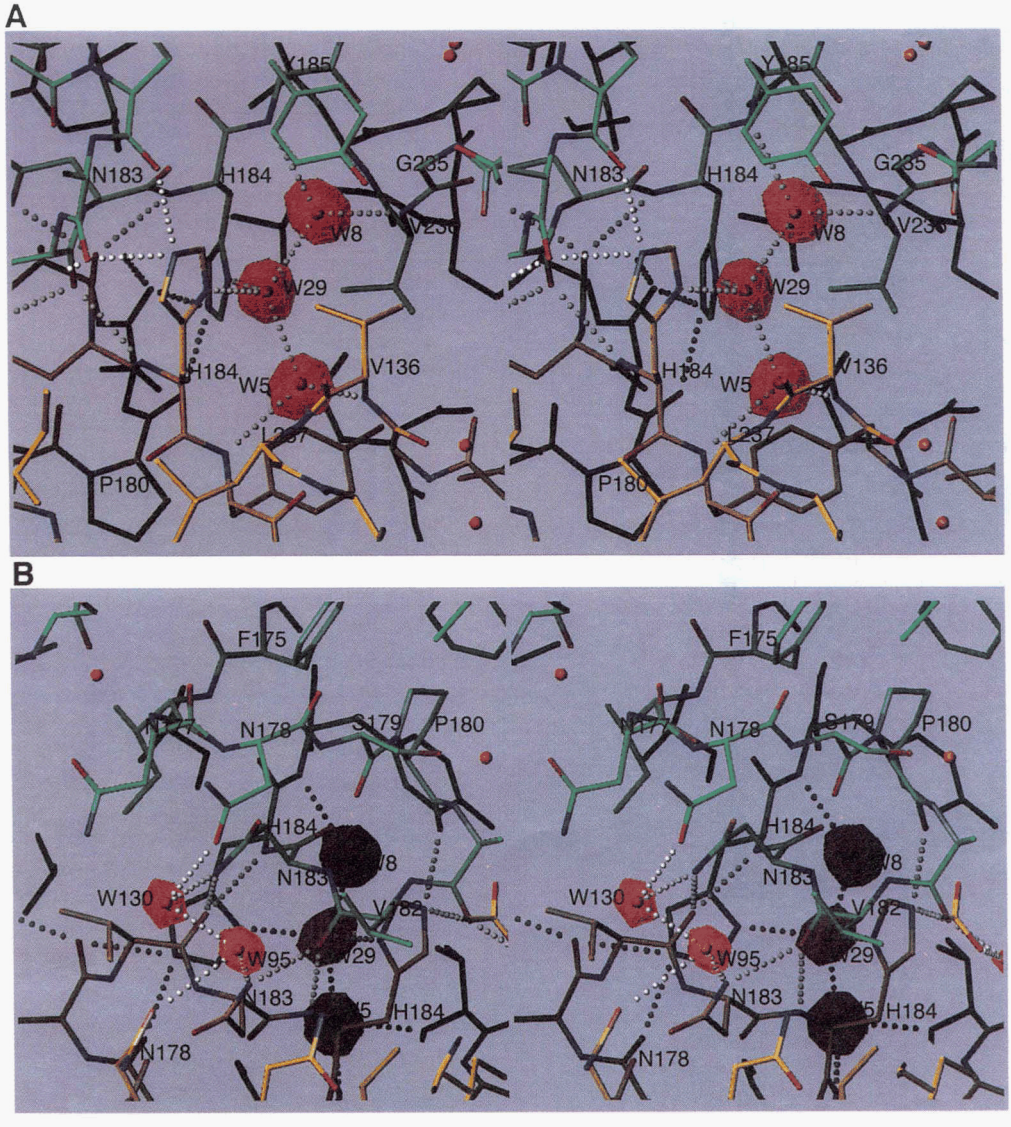

Fig. 5. Detailed views of two hydrogen bonding networks found in the dimer interface with monomer A in green and monomer B in yellow. Solvent atoms are depicted as small red spheres. **A:** Area near the core of the interface depicting the three buried waters in the core, shown with 5σ omit map difference density. **B:** Another hydrogen bonding network extending from the core to the periphery of the interface. The two bridging water molecules W-95 and W-130 have intermolecular hydrogen bonding angles near 90°. The same group of three solvent atoms shown in A can be seen in the background. This figure was created with O (Jones et al., 1991).

Electrostatic calculations indicate that the area surrounding the two active sites displays positive electrostatic fields, whereas the midsection is highly negative. A negatively charged polynucleotide substrate would be attracted to the ends and repelled by the midsection, thus directing the substrate and active sites to each other. Although the electrostatic fields of the monomers merge together in the midportion of the dimer, the two active sites have electrostatic fields that do not interact.

Our results suggest that both active sites of the *Serratia* endonuclease dimer should be able to independently cleave substrate. The orientation of the two active sites, however, is such that it seems unlikely that both could simultaneously interact with a single piece of nucleic acid. Rather, they would likely work independently on different pieces of nucleic acid or on very distant regions of the same substrate molecule if it were folded back on itself.

Advantages of a dimeric endonuclease

Dimerization for the *Serratia* endonuclease offers two distinct advantages over a monomeric protein. First, in the extracellular milieu where the enzyme produces nuclease acid nutrients, two active sites would increase the likelihood of an encounter with substrate. Simple dimerization has been shown in the case of triose phosphate isomerase to dramatically increase enzyme activity (Blacklow et al., 1988; Borchert et al., 1994). Second, the geometry of this dimer offers an additional advantage to the *Serratia* endonuclease by decreasing the angle of enzyme rota-

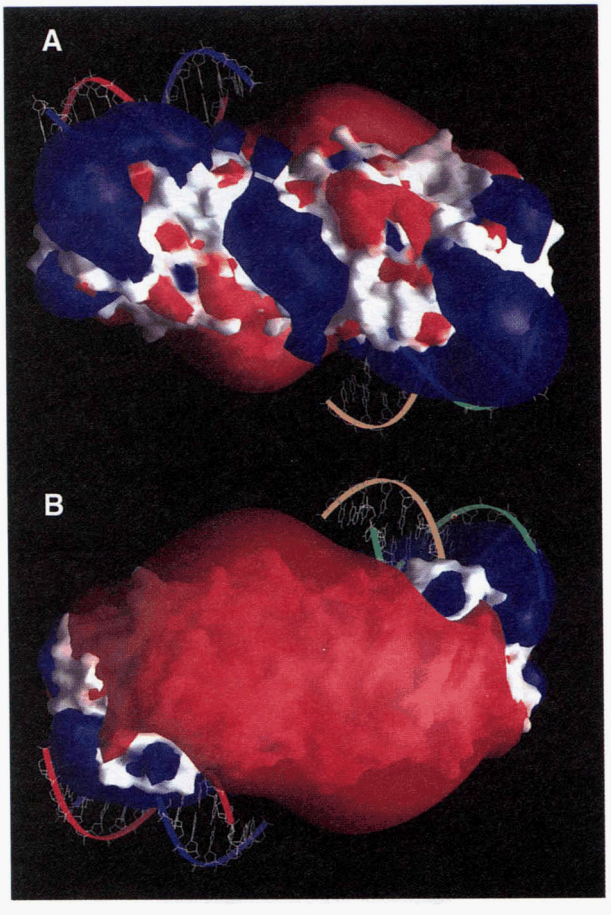

Fig. 6. Two views, rotated 180° relative to one another, of the nuclease dimer molecular surface with electrostatic contours at $\pm 1.2\ kT/e$ shown in blue and red, respectively. The two active sites of the dimer are located at both ends of the molecule in the region of positive (blue) electrostatic potential. To further illustrate the location and relative orientation of the two active sites, the B-DNA model of Miller et al. (1994) is shown superimposed. This figure was created with GRASP (Nicholls & Honig, 1992).

tion required to orient the enzyme into position to cleave substrate. The strong dipole of the *Serratia* nuclease monomer would require a maximum rotation of 180° to properly orient the active site with the substrate. With dimerization placing the two active sites on opposite sides of the molecule, a maximum rotation of only 90° would be required to align the nuclease with substrate. Other more general explanations of the advantages of multimeric proteins over monomeric proteins exist and involve theories of genetic parsimony or changes in their susceptibility to mutations (Goodsell & Olsen, 1993).

Further discussion

Other members of the class of sugar nonspecific nucleases, which includes the *Serratia* nuclease, are also thought to be homodimers, but sequence similarity with *Serratia* in the region of the dimer interface is not always present. For example, bovine endonuclease G and yeast mitochondrial nuclease (NUC1) are homodimers, but, when the nucleases are aligned (Friedhoff et al., 1994a), only 1 of the 16 residues listed in Table 3 as being important in dimer interactions is conserved in yeast. None of these residues are conserved in bovine. On the other hand, even though there is no mention of dimerization in the literature for the *Anabaena* nuclease (Muro-Pastor et al., 1992; 1994), this enzyme contains 5 of the 16 residues mentioned above in common with the *Serratia* endonuclease.

Future studies

Direct analysis of the effect of dimerization on the kinetics of *Serratia* endonuclease awaits the production of a monomeric form of the enzyme. Because we have now identified the important interactions found in the dimer interface, we can speculate that mutations that disrupt steric or electrostatic complementarity in the interface region might result in a monomeric protein. For example, replacement of His 184 with a large, bulky, charged residue, such as arginine, would affect both of these elements.

We would expect such a *Serratia* endonuclease monomer to be active because the active site is 25 Å removed from the dimer interface. Often monomers of naturally occurring dimers tend to be less stable and less active when compared with their dimeric form (Jaenicke, 1987), but a recently engineered monomeric form of TIM was found to be active despite loop rearrangements that move two catalytic residues out of position (Borchert et al., 1993). Although this result is very preliminary, we have produced small amounts of an active monomeric nuclease when we created a Ser 179 to Cys mutant to aid in the search for heavy atom derivatives. Light scattering experiments suggest that this mutant is monomeric in solution, but further characterization is pending. Interestingly, this mutant would not be expected to directly disrupt the dimer interface but the mutated residue is located near the interface.

Conclusion

We have found the *Serratia* nuclease to be a homodimer that forms through an isologous twofold interaction between residues in the carboxy-terminal subdomain. This dimerization preserves both accessibility to the active site and the electrostatic field, which can help align the enzyme and substrate. This is the first member of a family of sugar-nonspecific nucleases the structure of which has been solved. Further studies with substrate analogs, site-specific mutants, and co-crystallization with DNA should help to confirm these findings. In addition, results from studies with other members of this enzyme family should also aid in understanding this class of nucleases.

Experimental procedures

Source and purification of enzyme

The *Serratia* nuclease was purified from a genetically modified strain of *S. marcescens* by a procedure altered slightly from that published previously (Miller et al., 1991). The resulting nuclease was nearly homogeneous on SDS-PAGE and displayed normal activity in standard nuclease assays.

Light-scattering experiments

Dynamic light scattering was performed using a DynaPro 801 (Protein Solutions) with a 25-mW, 780-nm laser. Purified nuclease was concentrated to 10 mg/mL and dialyzed into the desired buffer. Several combinations of buffers (including 40 mM Tris, pH 8.2, 2 mM $MgCl_2$, 100 mM NaCl; 40 mM Tris, pH 8.2, 2 mM $MgCl_2$, 1 M NaCl; and 100 mM $NaPO_4$, pH 6.0) and protein concentrations (1–5 mg/mL) were used.

Crystal structure

The structure of the *Serratia* nuclease used in the analysis of the dimer was the 2.1-Å refined structure reported for the PEG crystals of Miller et al. (1994). These coordinates have been deposited with the Protein Data Bank (Bernstein et al., 1977) and have been assigned the identification code 1SMN. This structure has the same packing arrangement as the ammonium sulfate crystals reported by Miller et al. (1991) and should be similar to the crystal form reported by Bannikova et al. (1991). Both monomers in the asymmetric unit were treated independently in this refinement, that is, no noncrystallographic symmetry restraints, constraints, or averaging were used.

Structure analysis

Using a procedure similar to that used for the monomer (Miller et al., 1994), electrostatic field calculations were performed with GRASP and UHBD (Davis et al., 1991; Nicholls & Honig, 1992). The linearized Poisson–Boltzmann equation was solved by the finite difference method using a $65 \times 65 \times 65$ grid, which corresponds to a 1.3-Å spacing interval. All basic and acidic side chains were fully charged; histidines and all other atoms were set to neutral. The protein and solvent dielectric constants were set to 2 and 80, respectively, with an ionic strength of zero. The dielectric boundary was taken to be the molecular surface of the enzyme.

The systematic analysis of buried surfaces and intermolecular interactions in the crystal interfaces was performed using X-PLOR version 3.1 (Brünger, 1992) with the parhcsdx.pro parameter set from Engh and Huber (1991). This parameter set was also used in structure refinement. Energy calculations were done without a nonbonded cutoff or switching function and the dielectric constant was set to 2.0. The amount of solvent-accessible surface buried was taken to be the difference between sum of the surface area of the two interacting monomers in isolation and the surface area of the complex. To calculate the percentage of nonpolar and polar buried surface area, carbon and sulfur were classified as nonpolar and oxygen and nitrogen were considered polar (Lee & Richards, 1971). Hydrogen bonding and nonbonded contacts in the dimer interface were analyzed in Quanta v3.3 (Molecular Simulations Inc., 1992) and X-PLOR version 3.1. A 3.5-Å cutoff was used for all nonbonded interactions and the Baker and Hubbard (1984) criteria were used for hydrogen bonds. RMS differences between the atomic positions of the two monomers were calculated in X-PLOR version 3.1 after fitting the main-chain atoms from residues 8 to 244 of each monomer. The N- and C-terminal residues were omitted from the fit because they are not well resolved in the structure.

Acknowledgments

We thank Dr. J. Tanner for critical reading of the manuscript and Dr. M.J. Benedik for supplying a strain carrying the plasmid for nuclease overexpression. This work is supported in part by grants from the W.M. Keck Foundation, Robert A. Welch Foundation, National Institutes of Health, and the State of Texas. Some equipment used in this research was purchased through equipment grants from the National Science Foundation. M.D.M. is the recipient of an NIH predoctoral traineeship in the Houston Area Molecular Biophysics Program.

References

Aggarwal AK. 1995. Structure and function of restriction endonucleases. *Curr Opin Struct Biol 5*:11–19.

Baker EN, Hubbard RE. 1984. Hydrogen bonding in globular proteins. *Prog Biophys Mol Biol 44*:97–179.

Ball TK, Saurugger PN, Benedik MJ. 1987. The extracellular nuclease gene of *Serratia marcescens* and its secretion from *Escherichia coli*. *Gene 57*:183–192.

Bannikova GE, Blagova EV, Dementiev AA, Morgunova EY, Mikchailov AM, Shlyapnikov SV, Varlamov VP, Vainshtein BK. 1991. Two isoforms of *Serratia marcescens* nuclease: Crystallization and preliminary X-ray investigation of the enzyme. *Biochem Intl 24*:813–822.

Bernstein FC, Koetzle TF, Williams GJB, Meyer EF Jr, Brice MD, Rodgers JR, Kennard O, Shimanouchi T, Tasumi M. 1977. The Protein Data Bank: A computer-based archival file for macromolecular structures. *J Mol Biol 112*:535–542.

Biedermann K, Jepsen PK, Riise E, Svendsen I. 1989. Purification and characterization of a *Serratia marcescens* nuclease produced by *Escherichia coli*. *Carlsberg Res Commun 54*:17–27.

Blacklow SC, Raines RT, Lim WA, Zamore PD, Knowles JR. 1988. Triosephosphate isomerase catalysis is diffusion controlled. *Biochemistry 27*: 1158–1167.

Borchert TV, Abagyan R, Jaenicke R, Wierenga RK. 1994. Design, creation, and characterization of a stable, monomeric triosephosphate isomerase. *Proc Natl Acad Sci USA 91*:1515–1518.

Borchert TV, Abagyan R, Radha-Kishan KV, Zeeken JP, Wierenga RK. 1993. The crystal structure of an engineered monomeric triosephosphate isomerase, monoTIM: The correct modeling of an eight-residue loop. *Structure 1*:205–213.

Brünger AT. 1992. *X-PLOR version 3.1. A system for X-ray crystallography and NMR*. New Haven, Connecticut: Yale University Press.

Chothia C, Levitt M, Richardson D. 1981. Helix to helix packing in proteins. *J Mol Biol 145*:215–250.

Côté J, Renaud J, Ruiz-Carrillo A. 1989. Recognition of $dG_n \cdot dC_n$ sequences by endonuclease G: Characterization of the calf thymus nuclease. *J Biol Chem 264*:3301–3310.

Côté J, Ruiz-Carrillo A. 1993. Primers for mitochondrial DNA replication generated by endonuclease G. *Science 261*:765–769.

Creighton TE. 1993. *Proteins: Structures and molecular properties*. New York: WH Freeman & Co.

Davis ME, Madura JD, Luty BA, McCammon JA. 1991. Electrostatics and diffusion of molecules in solution: Simulations with the University of Houston Brownian dynamics program. *Comput Phys Commun 62*: 187–197.

Eaves GN, Jeffries CD. 1963. Isolation and properties of an exocellular nuclease of *Serratia marcescens*. *J Bacteriol 85*:273–278.

Engh RA, Huber R. 1991. Accurate bond and angle parameters for X-ray protein structure refinement. *Acta Crystallogr A 47*:392–400.

Filimonova MN, Baratova LA, Vospel'nikova ND, Zheltova AO, Leshchinskaya IB. 1981. Characterization of endonuclease from *Serratia marcescens*. *Biokhimiya 46*:1660–1666.

Filimonova MN, Krause KL, Benedik MJ. 1994. Kinetic studies of the *Serratia marcescens* extracellular nuclease isoforms. *Biochem Mol Biol Intl 33*:1229–1236.

Fraser MJ, Low RL. 1993. Fungal and mitochondrial nucleases. In: Linn SM, Lloyd RS, Roberts RJ, eds. *Nucleases, 2nd ed*. Cold Spring Harbor, New York: Cold Spring Harbor Laboratory Press. pp 171–207.

Friedhoff P, Gimadutdinow O, Pingoud A. 1994a. Identification of catalytically relevant amino acids of the extracellular *Serratia marcescens* endonuclease by alignment-guided mutagenesis. *Nucleic Acids Res 22*: 3280–3287.

Friedhoff P, Gimadutdinow O, Rüter T, Wende W, Urbanke C, Thole H, Pingoud A. 1994b. A procedure for renaturation and purification of the

extracellular *Serratia marcescens* nuclease from genetically engineered *Escherichia coli*. *Protein Expr Purif* 5:37–43.
Goodsell DS, Olsen AJ. 1993. Soluble proteins: Size, shape and function. *Trends Biochem Sci 18*:65–68.
Jaenicke R. 1987. Folding and association of proteins. *Prog Biophys Mol Biol 49*:117–237.
Janin J, Chothia C. 1990. The structure of protein–protein recognition sites. *J Biol Chem 265*:16027–16030.
Janin J, Miller S, Chothia C. 1988. Surface, subunit interfaces and interior of oligomeric proteins. *J Mol Biol 204*:155–164.
Jones S, Thorton JM. 1995. Protein–protein interactions: A review of protein dimer structures. *Prog Biophys Mol Biol 63*:31–65.
Jones TA, Zou JY, Cowan SW. 1991. Improved methods for building protein models in electron density maps and the location of errors in these models. *Acta Crystallogr A 47*:110–119.
Klotz IM, Langerman NR, Darnall DW. 1970. Quaternary structure of proteins. *Annu Rev Biochem 39*:25–62.
Kraulis PJ. 1991. MOLSCRIPT: A program to produce both detailed and schematic plots of protein structures. *J Appl Crystallogr 24*:946–950.
Lee B, Richards FM. 1971. The interpretation of protein structures: Estimation of static accessibility. *J Mol Biol 55*:379–400.
Matthews BW, Bernhard SA. 1973. Structure and symmetry of oligomeric enzymes. *Annu Rev Biophys Bioeng 2*:257–317.
Meiss G, Friedhoff P, Hahn M, Gimadutdinow O, Pingoud A. 1995. Sequence preferences in cleavage of dsDNA and ssDNA by the extracellular *Serratia marcescens* endonuclease. *Biochemistry 34*:11979–11988.
Miller MD, Benedik MJ, Sullivan MC, Shipley NS, Krause KL. 1991. Crystallization and preliminary crystallographic analysis of a novel nuclease from *Serratia marcescens*. *J Mol Biol 222*:27–30.
Miller MD, Tanner J, Alpaugh M, Benedik MJ, Krause KL. 1994. 2.1 Å structure of *Serratia* endonuclease suggests a mechanism for binding to double-stranded DNA. *Nature Struct Biol 1*:461–468.
Miller S. 1989. The structure of interfaces between subunits of dimeric and tetrameric proteins. *Protein Eng 3*:77–83.
Molecular Simulations Inc. 1992. *QUANTA, version 3.3*. Waltham, Massachusetts.
Monod J, Wyman J, Changeux JP. 1965. On the nature of allosteric transitions: A plausible model. *J Mol Biol 12*:88–118.
Muro-Pastor AM, Flores E, Herrero A, Wolk CP. 1992. Identification, genetic analysis and characterization of a sugar-non-specific nuclease from the cyanobacterium *Anabaena* sp. PCC 7120. *Mol Microbiol 6*: 3021–3030.
Muro-Pastor AM, Kuritz T, Flores E, Herrero A, Wolk CP. 1994. Transfer of a genetic marker from a megaplasmid of *Anabaena* sp. strain PCC 7120 to a megaplasmid of a different *Anabaena* strain. *J Bacteriol 176*: 1093–1098.
Nestle M, Roberts WK. 1969. An extracellular nuclease from *Serratia marcescens*: II. Specificity of the enzyme. *J Biol Chem 244*:5219–5225.
Nicholls A, Honig B. 1992. GRASP: Graphical representation and analysis of surface properties. New York: Columbia University.
Nyeste L, Sevella B, Holló J, Békés F. 1976. Kinetic study of extracellular nuclease of *Serratia marcescens*. *Eur J Appl Microbiol 2*:161–168.
Perutz MF. 1970a. Stereochemistry of cooperative effects in haemoglobin. *Nature 228*:726–734.
Perutz MF. 1970b. The Bohr effect and combination with organic phosphates. *Nature 228*:734–739.
Savage HFJ. 1993. Water structure. In: Westhof E, ed. *Water and biological macromolecules*. Boca Raton, Florida: CRC Press. pp 3–44.
Schmitz KS. 1990. *An introduction to dynamic light scattering by macromolecules*. Boston, Massachusetts: Academic Press.
Tsai CJ, Jorden KD. 1993. Theoretical study of small water clusters: Low-energy fused cubic structures for H_2O_n, $n = 8$, 12, 16, and 20. *J Phys Chem 97*:5208–5210.
Vincent RD, Hofmann TJ, Zassenhaus HP. 1988. Sequence and expression of *NUC1*, the gene encoding the mitochondrial nuclease in *Sacchromyces cerevisiae*. *Nucleic Acids Res 16*:3297–3312.
Yonemura K, Matsumoto K, Maeda H. 1983. Isolation and characterization of nucleases from a clinical isolate of *Serratia marcescens kums* 3958. *J Biochem 93*:1287–1295.
Zielenkiewicz P, Rabczenko A. 1984. Protein–protein recognition: Method for finding complementary surfaces of interacting proteins. *J Theor Biol 111*:17–30.